

Cytotoxicity and Specificity of Directed Toxins Composed of Diphtheria Toxin and the EGF-like Domain of Heregulin $\beta 1$ [†]

Ralf Landgraf,[‡] Mark Pegram,[§] Dennis J. Slamon,[§] and David Eisenberg^{*‡}

Department of Chemistry and Biochemistry and Division of Hematology-Oncology, University of California—Los Angeles, Box 951570, Los Angeles, California 90095-1570

Received September 18, 1997; Revised Manuscript Received December 29, 1997

ABSTRACT: As a step in the design of directed toxins, aimed at cells that overexpress HER receptors, particularly breast carcinoma cells, we studied the properties of a chimera of diphtheria toxin (DT) and heregulin $\beta 1$. The EGF-like growth hormone heregulin is a ligand for the HER3 and HER4 receptors and their heterodimers with HER2. The 60-residue EGF-like domain (hrg) of heregulin elicits a biological response and binds to these receptors primarily through its N terminus. We tested a fusion protein in which hrg replaces the C-terminal receptor-binding domain of DT (DT(389)hrg) and an alternative design in which this domain is fused to the N terminus of DT(389). Of those two constructs, the N-terminal fusion was not active as a directed toxin but elicited a growth response. The C-terminal fusion of hrg to DT(389) yielded a functional toxin and showed cell line specific cytotoxicity that is consistent with heregulin specificity. The binding of hrg to its cognate receptor is not impaired as shown by receptor activation, direct binding, and competition with free hrg. Cytotoxicity is dependent on high-affinity binding of DT-(389)hrg to HER3 and HER4 receptors and is not mediated by HER2 overexpression alone. For those cell lines exhibiting high-affinity binding sites, the level of cytotoxicity correlates with the rate of internalization. Thus DT(389)hrg chimeras offer a possible avenue toward directed toxins against cells that overexpress HER receptors.

Directed toxins have been under intense investigation for their usefulness in cancer treatment. The classic directed toxin consists of a peptide ligand that binds to specific cell surface targets, fused to a toxin's catalytic and translocation domains. Such a peptide ligand can be the free-standing domain of an antibody, resulting in an immunotoxin, or a peptide hormone. Toxins that have been tested in this context include diphtheria toxin, *Pseudomonas aeruginosa* exotoxin A, and blocked ricin A chains (1–3).

The directed toxin used in this study includes domains of diphtheria toxin (DT). Diphtheria toxin of *Corynebacterium diphtheriae* is a potent killer of eukaryotic cells. The 535-residue protein consists of three domains, one for each function of this protein (4) (Figure 1). The 187 amino acid long catalytic (C) domain is responsible for the ADP ribosylation of eukaryotic elongation factor 2 upon cell entry, which brings protein synthesis to a halt and ultimately leads to cell death. Cell entry is facilitated through the translocation (T) domain (residues 199–379) in the acidic environment of an endosome. The nature of this translocation mechanism is not fully understood. The initial binding to the DT receptor, the heparin binding EGF-like growth factor precursor (5), is the function of the C-terminal receptor-binding (R) domain. This modular design of DT has facilitated the construction of directed toxins. The receptor-

binding domain of DT has been replaced with cell specificity conferring ligands such as luteinizing hormone (6), interleukin 4 (7), interleukin 2 (8), and fibroblast growth factor 6 (9).

We chose the EGF-like growth hormone heregulin to direct the toxic activity of diphtheria toxin. Heregulin was initially thought to be the ligand for the EGF receptor homologue HER2 (cErbB2 or HER2/neu) but has since been shown to require heterodimerization with the related HER3 or HER4 receptors for high affinity binding (10). The overexpression of HER2 in more than 30% of human breast carcinoma (11) and the implication of overexpressed HER3 or HER4 in cellular transformation (12) have created an interest in heregulin as a possible targeting device for various forms of cell line specific cancer treatments. More than 10 isoforms of heregulin (also termed acetylcholine receptor inducing activity (ARIA), neu differentiation factor (NDF), glial growth factor (GGF), or neuregulin) have been identified. Heregulin is expressed in a variety of tissues, but tissue-specific isoforms (such as GGF or ARIA) exist. Multiple isoforms (α , $\beta 1$, $\beta 2$, $\beta 3$) are derived from a single gene by alternative splicing (13). A second heregulin-like gene (neuregulin 2) has recently been identified which undergoes similar alternative splicing (14, 15). The different isoforms of heregulin are either secreted directly or generated as longer precursors with a putative transmembrane region and may yield the soluble portion by proteolytic cleavage (13, 16). The soluble forms of heregulin (approximately 240 amino acids) contain both an immunoglobulin-like domain and an EGF-like domain. The 60 amino acid EGF-like domain (hrg) of heregulin is sufficient for receptor binding and provides a small and compact targeting moiety which can be used in

[†] This work was supported by the National Institutes of Health [Grants GM31299 (D.E.) and 1K12 CA01714 (M.P.)] and the Department of Defense Breast Cancer Research Program [Grant DAMD 17-94-J-4234 (D.J.S.)].

^{*} To whom correspondence should be addressed.

[‡] Department of Chemistry and Biochemistry.

[§] Division of Hematology-Oncology.

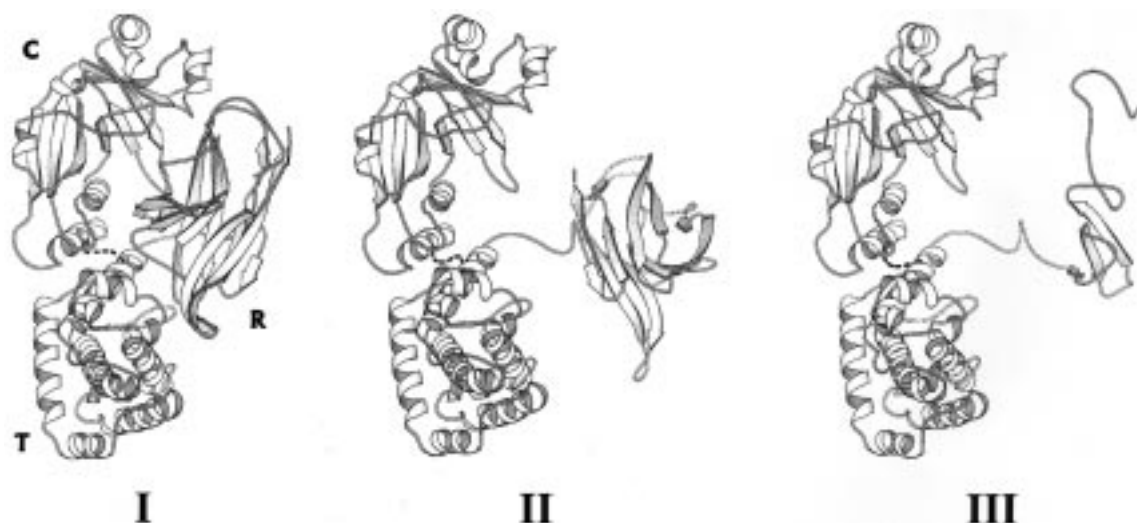


FIGURE 1: Crystal structure of the closed (I) and open (II) forms of diphtheria toxin compared with a model for the chimeric toxin DT-(389)hrg (III). The catalytic (C), translocation (T), and receptor-binding (R) domains have been indicated in the closed form of DT. For the DT(389)hrg model the structure of the hrg domain, as solved by NMR (23), has been combined with the structure of the catalytic and translocation domains through the connecting loop as it is found in the open form of DT. The model was created using Insight II (Biosym), and the graphics were generated using Molscript (38).

the design of directed toxins. We used this 60 amino acid domain in the design of DT-hergulin chimeras.

By fusing hrg to DT, it is our goal to turn DT into a directed toxin, aimed at carcinoma cells that overexpress HER receptors. The design of such a DT-hergulin chimera is complicated by the fact that the N terminus of the hrg domain has been identified as the single most important region for receptor binding (17). Tight binding by this portion of the molecule has been attributed mainly to the interaction with HER3 or HER4. In several instances the hrg domain has been used as a targeting moiety for PE40-based directed toxins (18–20), thereby keeping those residues N-terminal. However, the order of domains in the diphtheria toxin gene places the receptor-binding domain C-terminal of the C and T domains. Figure 1 shows the three-dimensional structure of diphtheria toxin in its closed and open forms. The open form is found in domain-swapped dimers of DT (21) and in the complex of DT with its natural receptor (22). A model based on the open form of DT and the NMR structure of hrg (23) suggests that the open form of DT can accommodate hrg at its C terminus without obvious steric interference. However, the binding of the N terminus of hrg to its cognate receptor might still be impaired. Alternatively, hrg can be fused to the N terminus of DT, thereby avoiding any possible interference with hrg receptor binding. This order of functional domains differs from that found in wild-type DT. It has been shown that proteins fused to the N terminus of DT can be cotranslated to the cytosol (24). The purpose of this work was therefore to identify the best design for a functional directed toxin based on the C and T domains of DT (DT(389)) and hrg and to evaluate its cytotoxic and binding properties.

EXPERIMENTAL PROCEDURES

Construction of the DT(389)hrg Construct. The 60 amino acid EGF-like domain of human heregulin $\beta 1$ (amino acids 177–236) was generated by a series of overlapping oligonucleotides, amplified by PCR, and cloned into the *EcoRI* and *HindIII* sites of the pET32-a expression vector (Novagen,

Madison, WI). The sequence of the hrg clone was confirmed, and expressed hrg was tested for its ability to stimulate the tyrosine phosphorylation of HER2. The diphtheria toxin fragment 1–389, containing the catalytic and translocation domains, was amplified by PCR from the *C. diphtheria* strain CRM45, kindly provided by Dr. John R. Murphy (Boston University, MA). CRM45 harbors a naturally occurring mutant of DT that lacks the receptor-binding domain. DT(389) was amplified with an N-terminal *MfeI* site and a C-terminal *EcoRI* site and was inserted into the *EcoRI* site at the hrg N terminus in pET32a/hrh. For the DT(389) control, a stop codon was introduced immediately adjacent to the C-terminal *EcoRI* site. Two-step PCR was used to generate hrg-DT(389) from those two clones. The coding regions of DT(389) and hrg were confirmed by sequencing.

Purification of Chimeric Toxins. The three chimeric toxins were expressed in *Escherichia coli* BL21(DE3) cells as a thioredoxin fusion protein and were purified on a 5-mL Pharmacia “HITRAP Chelating” column, loaded with NiSO_4 . The eluted protein was concentrated and dialyzed against 50 mM Tris (pH 8.0). CaCl_2 was added to 10 mM and Tween 20 to 0.1% prior to proteolytic cleavage. Cleavage was carried out for 20 h at room temperature with 1 unit of enterokinase (Invitrogen, San Diego, CA) for every 3 mL of protein solution. The cleaved chimeric toxins were removed from residual uncleaved starting material during a second run on a Ni-chelating column. The flow-through was applied to a Q2 anion exchange column (BioRad, Hercules, CA) after dialysis against 50 mM Tris, pH 9.0. The final protein was eluted in a 50–500 mM NaCl gradient and was free of impurities based on SDS-PAGE and Coomassie staining.

Tyrosine Phosphorylation Assay. MCF-7 cells, obtained from the American Type Culture Collection (Rockville, MD), were grown to 80% confluence in 100 mm² culture dishes in RPMI 1640 medium supplemented with 10% heat-inactivated fetal bovine serum, 2 mM glutamine, and 1% penicillin G–streptomycin–fungizone solution (Irvine Sci-

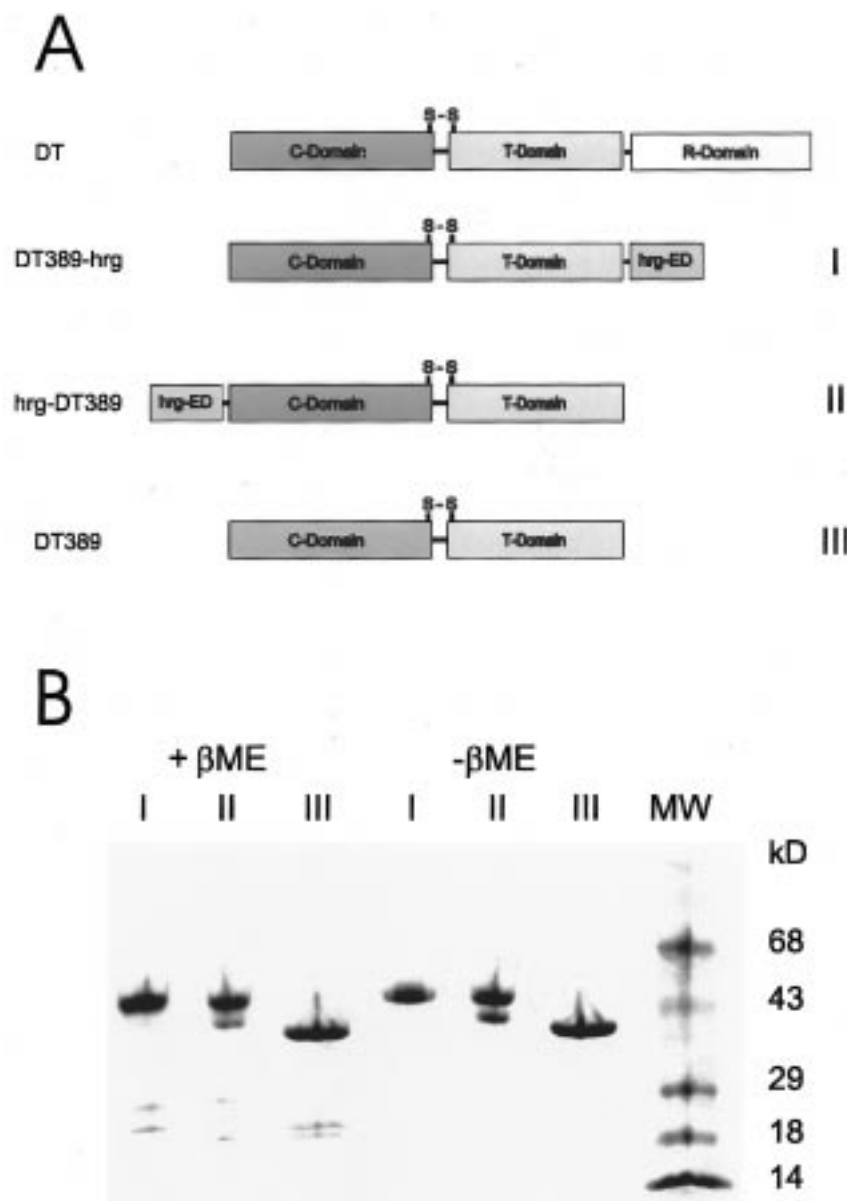


FIGURE 2: Design of the chimeric toxins used in this study. (A) Diphtheria toxin (DT) compared to the chimeric toxins containing a C-terminal (I) or N-terminal (II) hrg domain. Construct III was used as the negative control for hrg-independent binding. The C and T domains of DT are held together by a disulfide bridge even after proteolytic cleavage of the flexible linker region. (B) SDS-PAGE gel of constructs I–III with (left side) and without (right side) β -mercaptoethanol to illustrate partial nicking at the linker region between the C and T domains. The content of each lane is indicated on top.

entific, Santa Ana, CA). Following serum starvation for 24 h, 50 nM DT(389)hrg or control solution was added to 2 mL of serum-free RPMI medium for the time points indicated in Figure 3. Cells were lysed at 4 °C in 0.6 mL of lysis buffer (20 mM Tris, pH 8.0, 137 mM NaCl, 1% Triton X-100, 10% glycerol, 5 mM EDTA, 1 mM sodium orthovanadate, 1 mM phenylmethyl-sulfinyl fluoride, leupeptin 1 μ g/mL, and aprotinin 1 μ g/mL). Insoluble material was cleared by centrifugation at 10000g for 10 min, and the resulting protein was quantitated using BCA (Pierce Biochemicals, Rockford, IL). For the direct analysis of tyrosine phosphorylation, 10–50 μ g of protein lysate was analyzed by SDS-PAGE, transferred to a PVDF membrane (Millipore, Bedford, MA), and probed with mouse-anti-phosphotyrosine antibodies (SC508, Santa Cruz Biotechnology, Santa Cruz, CA). HRP-conjugated anti-mouse antibodies (SC2005) were used for detection by chemiluminescence. For the

analysis of HER2 tyrosine phosphorylation, cell lysates were immunoprecipitated by incubating 250 μ g protein with 5 μ g/mL monoclonal anti-HER2 antibodies (Oncogene Science, Uniondale, NY) at 4 °C for 18 h with gentle agitation. Protein A-agarose (BioRad, Hercules, CA) was added to precipitate the antigen-antibody complex, and the immunoprecipitates were washed three times in lysis buffer prior to SDS-PAGE.

Cell Proliferation Assay. Twenty-four hours prior to exposure to the toxin, 96-well plates were seeded with 5000 cells/well in RPMI medium. The medium was exchanged for RPMI including different concentrations of chimeric toxins, and the cells were incubated for 72 h at 37 °C in a humidified atmosphere containing 5% CO₂. For the timed experiments, toxin exposure was terminated at the times indicated in Figure 4. The cells were washed twice with sterile PBS and were allowed to incubate the remaining 72

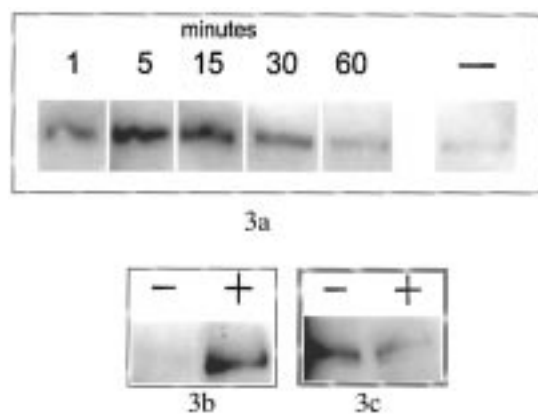


FIGURE 3: Tyrosine phosphorylation of HER2 as a result of stimulation with DT(389)hrg. (a) Western blot analysis of tyrosine phosphorylation in MCF-7 cells after different time points of stimulation. Cells were stimulated with 50 nM DT(389)hrg for the time indicated on top of each lane. (b) HER2 is phosphorylated in response to DT(389)hrg stimulation. Anti-phosphotyrosine Western blot of MCF-7 cell lysate after immunoprecipitation with anti-HER2 antibodies. MCF-7 cells were lysed after 5 min in the presence (+) or absence (-) of 50 nM DT(389)hrg in the media. (c) Increased tyrosine phosphorylation is accompanied by HER2 down regulation. The Western blot shown in Figure 3b was reprobed with anti-HER2 antibodies.

h. The number of adherent cells after 72 h of incubation was determined by staining with N-hexamethylpararosaniline as described (25, 26).

Protein Synthesis Inhibition Assay. The protein synthesis inhibition assay is a modification of the method described

by Carroll et al. (27). Twenty-four-well plates were seeded at a density of 200 000 cells/well and were allowed to adhere for 24 h in RPMI medium. Adherent cells were then allowed to incubate with chimeric toxin at the various concentrations for 12 h. Following toxin exposure, the medium was removed, cells were washed twice with leucine-free MEM (Eagle), and 300 μ L of leucine-free MEM, containing 1 μ Ci of 3 H-leucine/mL, were added for 2 h at 37 $^{\circ}$ C. Following the 3 H-leucine incorporation, cells were washed twice with MEM and solubilized in 300 μ L of lysis buffer (0.5% SDS, 1 mM MgCl_2 , 1 mM CaCl_2). Proteins were precipitated from this lysate with 50 μ L of TCA (60%), and the pellet of the centrifugation was washed with 10% TCA, resolubilized in 0.5 M NaOH, and counted.

Iodination of DT(389)hrg. To 100 μ L of PBS (pH 6.5), containing 5 μ g of DT(389)hrg and 0.5 mCi of $\text{Na } ^{125}\text{I}$ (Amersham, Arlington Heights, IL), one IODO-Bead (Pierce, Rockford, IL) was added to start the iodination reaction. After 15 min at room temperature, the IODO-Bead was removed, and free label was separated on a PD10 desalting column (Pharmacia, Piscataway, NJ). The final labeled protein had a specific activity of 150 000 cpm/ng and was stored at 4 $^{\circ}$ C in PBS.

Cell-Binding Assay. The various cells listed in Figure 4 were grown to approximately 80% confluence in 75-cm² tissue culture flasks and were removed from the flasks through treatment with Versene (BRL, Grand Island, NY). The cells were washed once with ice-cold PBS and resus-

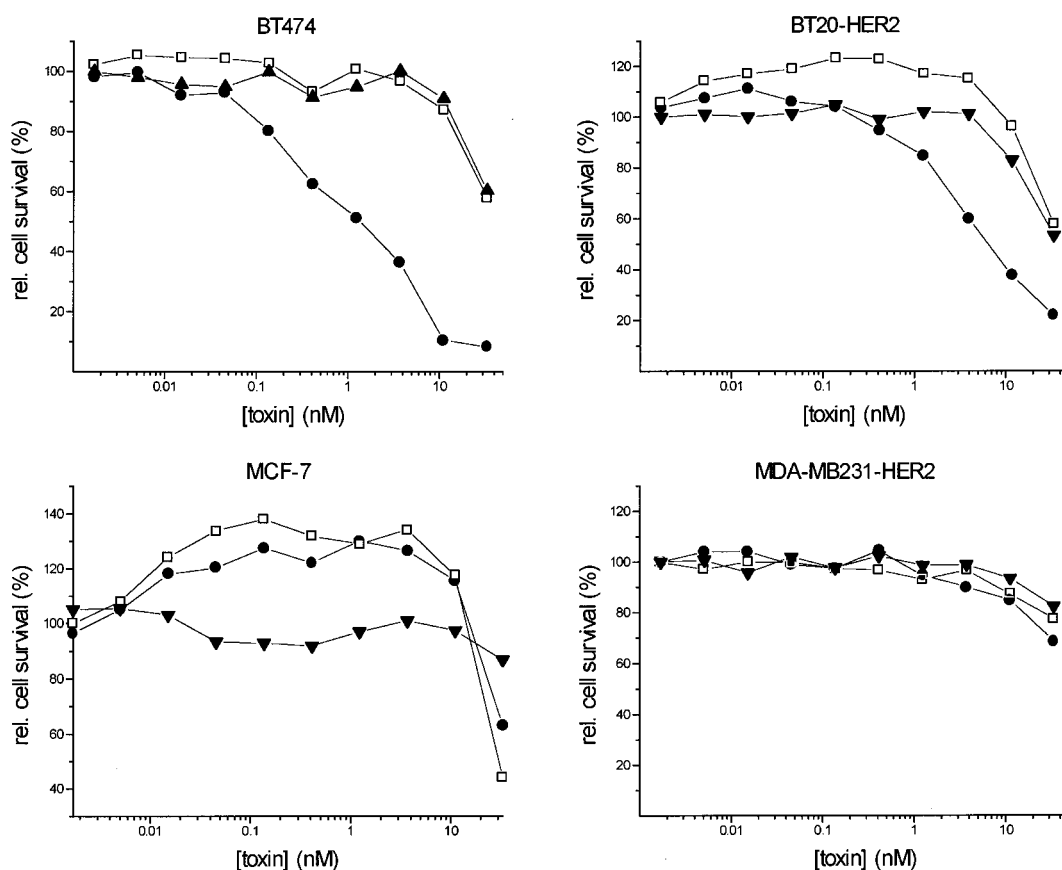


FIGURE 4: DT(389)hrg acts as a functional, hrg-directed toxin. The cytotoxicity of the chimeric toxins of Figure 2 toward various cell lines is plotted as the percentage of cell survival relative to the untreated control after 3 days of growth in the presence of three chimeric toxins (DT(389)hrg = \bullet , hrgDT(389) = \square , and DT(389) = \blacktriangle). The cell lines used for each assay are indicated above each graph. Cell lines marked "HER2" have been transfected with and overexpress HER2.

pended in PBS at 10^6 cells/mL; 10^5 cells ($100\ \mu\text{L}$) were incubated at $4\ ^\circ\text{C}$ with $50\ \mu\text{L}$ of unlabeled DT(389)hrg (or hrg) at various concentrations and with $50\ \mu\text{L}$ of PBS containing 3 ng (450 000 cpm) of ^{125}I -labeled DT(389)hrg. After 2 h at $4\ ^\circ\text{C}$ with gentle agitation, cells were spun down (4 min at 5000 rpm) and the supernatant was collected. The pellet was washed once with $750\ \mu\text{L}$ of cold PBS. The supernatant (displaced) fraction and pellet (bound fraction) were counted in a gamma counter. For the Scatchard representation of data, the displaced counts were used to plot bound/free as a function of the free competitor. Binding data are the averages of three reactions for each concentration.

Internalization Assay. Twenty-four-well plates were seeded with the cells indicated in Figure 6 at 60 000 cells/well in RPMI medium 24 h prior to the experiment. Plate-adherent cells were washed twice with ice-cold PBS and incubated at $4\ ^\circ\text{C}$ with $200\ \mu\text{L}$ of ice-cold binding medium (MEM + 0.1% BSA). Control reactions contained 500 ng of cold DT(389)hrg in the binding medium. After 1 h, $100\ \mu\text{L}$ of binding medium, containing $1\ \mu\text{L}$ of labeled DT-hrg (3 ng), was added, and the incubation was continued at $4\ ^\circ\text{C}$ for 1 h. To initiate endocytosis, the cells were moved to $37\ ^\circ\text{C}$ in a humidified atmosphere containing 5% CO_2 for the length of time indicated in Figure 6. At the indicated time, cells were placed at $4\ ^\circ\text{C}$ and the supernatant was removed. The cells were washed twice with ice-cold PBS and incubated with $200\ \mu\text{L}$ of PBS (adjusted to pH 8) and 0.1 mg/mL proteinase K (Sigma, St. Louis, MO) for 1 h at $4\ ^\circ\text{C}$. The supernatant was cleared by centrifugation (3 min, 5000 rpm) to remove dislodged cells and was counted as the bound, noninternalized fraction. The pellet of the centrifugation was combined with the SDS lysate (0.1 N NaOH, 0.1% SDS for 5 min at $37\ ^\circ\text{C}$) of cells still attached to the plate after two PBS washes (internalized fraction). Counts obtained in the presence of a 500-fold excess of cold DT(389)hrg (less than 5%) were subtracted as nonspecifically bound and internalized DT(389)hrg.

RESULTS

To evaluate designs for a chimeric toxin, consisting of the diphtheria toxin catalytic and translocation domains and the hrg domain, we generated three different constructs (Figure 2A). The truncated form of the toxin (DT(389)), which lacks the receptor-binding domain, was generated as a negative control for cytotoxicity that is not mediated by the binding of hrg to its cognate receptor. We generated two chimeric toxins in which the hrg domain was located either N-terminal of DT(389) (construct II, hrg-DT(389)) or C-terminal of DT(389) (construct I, DT(389)hrg). All three constructs were expressed in the cytoplasm of *E. coli* as soluble thioredoxin fusion proteins.

The purification of all three DT constructs was accompanied by partial nicking (Figure 2B). The resulting fragments are consistent with the arrangements of subunits indicated in Figure 2A. The three domains in DT are linked through two flexible linker regions. The linker region between the C and T domains is exceptionally labile to proteolysis and is readily nicked by trypsin. Under *in vivo* conditions, the nicking of this linker takes place at the cell surface by target cell proteases and has to occur for the

successful transfer of the catalytic domain to the cytosol of the target cell (28). The resulting fragments are held together by the indicated disulfide bridge (Figure 2A) until the C domain is released into the cytosol. The location of this cleavage site between the C and T domains can be confirmed by SDS-PAGE under oxidizing conditions. Under those conditions, both fragments remain covalently associated (Figure 2B). During purification, all three constructs exhibit a comparable level of susceptibility to proteolysis at this linker region. Since proteolysis at this site is an intrinsic part of DT intoxication, it does not impair the use of these constructs as directed toxins.

The second flexible linker region in DT joins the T and R domains. In the closed form of DT the R-domain is tightly packed against the C and T domains (4). A model of DT(389)hrg based on the closed form of DT revealed that the hrg domain cannot be readily accommodated without structural changes in either component or an opening of this linker region. The working model presented in Figure 1 (III) was therefore based on the open form of DT, found in domain-swapped dimers (21) and, in a similar form, in its complex with the DT receptor (22).

In the reversed hrg-DT(389) construct the C terminus of hrg is connected to the N terminus of DT(389). During purification, this construct exhibits a high degree of susceptibility toward proteolysis, and the strong band in Figure 2B (construct II $\pm\ \beta$ -mercaptoethanol) at a molecular weight just above the DT(389) control is probably due to cleavage in this linker region. The flexible portion of this linker consists mainly of the C terminus of hrg. According to the NMR structure of hrg (23), the C terminus is relatively flexible. It lacks the stabilization which the N-terminal receptor-binding region receives through β -sheet formation and three disulfide bridges. A high level of nicking at this site will result in free hrg and untargeted toxin and will reduce the effectiveness of the directed toxin. Therefore, with respect to the stability of this second linker region between DT(389) and the hrg domain, DT(389)hrg is superior to the hrg-DT(389) construct.

To test the availability of the receptor-binding N terminus of the hrg domain to bind to its cognate receptor, we measured the ability of this chimeric toxin to stimulate tyrosine phosphorylation of HER2 in MCF-7 parental cells. MCF-7 parental cells do not express heregulin, do exhibit a low level of heregulin-independent tyrosine phosphorylation, and do respond well to stimulation by heregulin (25). Figure 3a shows a time course of tyrosine phosphorylation of a 185-kD protein in response to DT(389)hrg stimulation. This fast response is comparable to the published time course of heregulin-induced tyrosine phosphorylation of HER2 in T47D human mammary carcinoma cells (29). To confirm the identity of the phosphorylation signal shown in Figure 3a, we subjected the MCF-7 cell lysate to immunoprecipitation with anti-HER2 antibodies prior to Western blot analysis with anti-phosphotyrosine antibodies (Figure 3b,c). This analysis confirms that stimulation with DT(389)hrg results in increased levels of tyrosine-phosphorylated HER2 within 5 min (Figure 3b), while the overall levels of HER2 decrease upon stimulation (Figure 3c). This DT(389)hrg-dependent tyrosine phosphorylation of HER2 demonstrates that the hrg domain in this chimeric toxin construct is in a

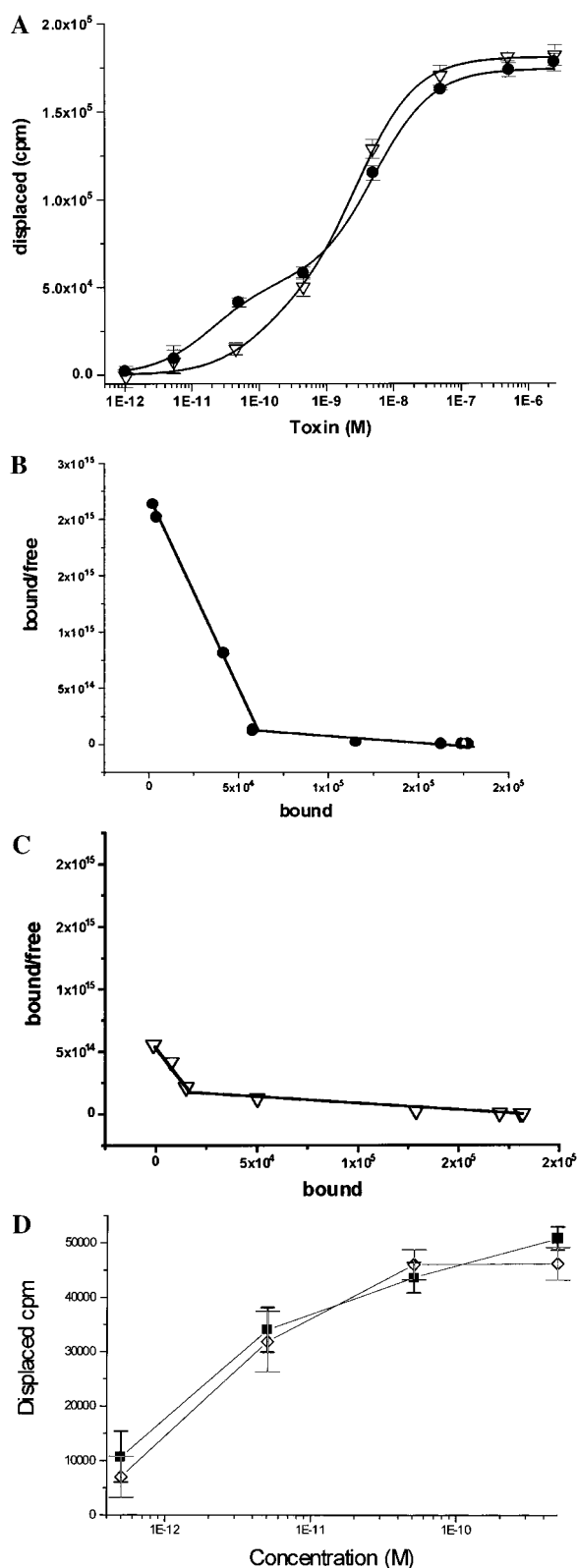


FIGURE 5: Binding of DT(389)hrg to target cell lines. (A) Binding of DT(389)hrg to BT20-HER2 (●) and MDA-MB231-HER2 (▽) cells. The displaced [125 I]-DT(389)hrg is shown as a function of the concentration of unlabeled DT(389)hrg. (B) Scatchard plot of DT(389)hrg binding to BT20-HER2 cells indicating the presence of low- and high-affinity binding sites. (C) Scatchard plot of DT(389)hrg binding to MDA-MB231-HER2 cells showing a substantially reduced high-affinity component compared to BT20-HER2 cells. (D) Displacement of [125 I]-DT(389)hrg from the high-affinity binding site of BT20-HER2 cells by DT(389)hrg (■) or free hrg (◇).

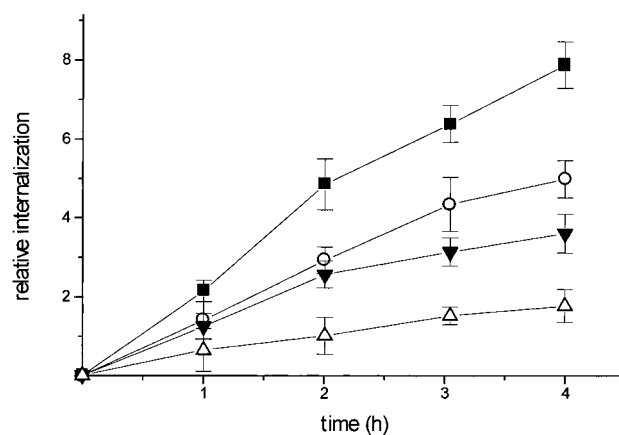


FIGURE 6: Target cell lines differ in their rate of [125 I]-DT(389)-hrg internalization. The relative internalization of [125 I]-DT(389)-hrg is shown as the ratio of internalized cpm at the indicated time points to surface-bound cpm at time 0. The relative internalization is presented for four different cell lines. (BT474 = ■, BT20-HER2 = ○, MCF-7 = ▽, and MDA-MB231-HER2 = △).

biologically active form and the receptor-binding N terminus is accessible to the hrg cognate receptor.

Having confirmed the biological activity of the hrg domain in DT(389)hrg, we analyzed the biological activity of the toxin component using two independent assays. The first assay measures cytotoxicity over a period of 3 days in the presence of the toxin. The second assay is more specific to the mechanism by which DT elicits cellular toxicity. It measures the inhibition of protein synthesis resulting from the ADP-ribosylation of elongation factor 2 by the catalytic subunit of diphtheria toxin. We selected five cell lines for these assays on the basis of their levels of expression of the different HER receptors. The negative control cell line MDA-MB231-HER2 was chosen because of its failure to respond with tyrosine phosphorylation of HER2 upon stimulation by hrg (25). Furthermore, related cell lines had previously been tested for their sensitivity to hrg-PE40 chimeric toxins. Using two independent assays, this panel of cell lines gives us the option to compare the relative order of these cells in terms of toxin sensitivity for the DT- and PE40-based constructs.

First, we analyzed the different toxins for their cytotoxic effect on the selected cell lines. The five different cell lines show very different responses to the toxin. Four of the five cell lines with distinct dose response patterns are presented in Figure 4. The results for CaOV3-HER2 cells are qualitatively intermediate to BT20-HER2 and MCF-7 and are listed only numerically in Table 1. BT474 shows the strongest response to the DT(389)hrg toxin with a 50% inhibition of cell growth at a concentration of 1 nM. A concentration of approximately 50 nM is required for the reversed toxin construct (hrg-DT(389)). The toxicity at this higher concentration matches that observed for the negative control (DT(389)). Among the cell lines responsive to the toxin, BT474 stands out by apparently responding only with growth inhibition, whereas BT20-HER2 and MCF-7 exhibit both growth stimulation at low concentrations and growth inhibition at higher concentrations. The MDA-MB231-HER2 cells used in this analysis fail to respond to either toxin construct. This resistance is consistent with their reported failure to respond to hrg, as judged by HER2 phosphorylation (25). On the basis of the results of the

Table 1: Summary of Toxicity Data for DT(389)hrg and Comparison of HER Receptor Presentation^a

cell line	rel abundance of receptors			IC(50) (nm)		internalization (turnover/h)	
	HER2	HER3	HER4	DT(389)hrg	hrg-PE40	initial	% at 4 h
BT474 ^b	+++	++	+++	1	0.02 ^b	2.11	74
BT20-HER2 ^c	++++	++	+++	5	1–2 ^c	1.41	47
CaOV3–HER2	++++	+++	+	10–12	na ^d	nd ^e	nd
MCF7 ^b	+/-	+++	+	22	2.5 ^b	1.24	40
MDA-MB231-HER2 ^c	++++	+	–	>30	>40 ^c	0.65	40

^a The relative abundance of each receptor is indicated relative to its maximum abundance on breast and ovarian epithelial cells (i.e., levels marked “+++” for HER2 are not equivalent to levels marked “+++” for HER4 in terms of the absolute numbers of receptors). The data on receptor presentation for the parental cell lines and hrg-PE40 toxicity were taken from the references on the corresponding hrg-PE40 constructs (Jeschke et al. (19) Siegal et al. (10)). The relative ratios for HER2 overexpressing cells have been independently determined in our laboratory by quantitative Western blot analysis (37 and data not shown). The IC(50) for DT(389)hrg is based on the growth inhibition assay. The rate of internalization is given as the slope in Figure 6. The rate of internalization observed after 4 h is given as a percentage of the initial rate. ^b Reference 30. ^c Reference 19. ^d Not applicable. ^e Not determined.

cytotoxicity assay, the fusion of hrg to the C terminus of DT(389) creates a functional toxin in which the hrg domain is able to interact with its cognate receptor, and the remaining DT domains are biologically active. A comparison with data reported for chimeras of *Pseudomonas* exotoxin A and hrg shows that the relative order of cell lines with respect to their cytotoxic response to DT(389)hrg matches the combined findings for hrg-PE40 constructs from different sources (18–20).

On the basis of the cytotoxicity assay, the fusion of hrg to the N terminus of DT(389) does not yield a functional toxin and behaves similarly to the non-hrg-targeted control toxin (DT(389)). The toxicity at the level of DT(389) verifies that the catalytic and probably the translocation domains are functional. The growth stimulation observed for BT20-HER2 and MCF-7 suggests that the hrg domain is able to bind and activate cell surface receptors. One possible explanation for the lack of directed toxicity by this reversed construct would be rapid proteolysis in situ, resulting in DT(389) and free hrg.

To expand upon the results obtained from the cytotoxicity assay, we measured the activity of the toxin by monitoring the inhibition of protein synthesis. Protein synthesis was measured after 12 h of exposure to the toxin by counting the [³H] leucine incorporated over a period of 2 h. The results of this analysis (data not shown) confirm the findings of the cell proliferation assay, with respect to both the concentrations of chimeric toxin required to achieve 50% inhibition and the relative sensitivity of the tested cell lines.

The relative sensitivity of different cell lines to hrg-based chimeric toxins has been correlated previously to the presence of the high-affinity binding sites provided by HER4 and to a lesser extent HER3 (19, 30). To correlate the binding of DT(389)hrg to the tested cell lines with the observed toxicity, we carried out binding studies using ¹²⁵I-DT(389)hrg. In our studies all cell lines exhibited a low-affinity binding site ($K_d \sim (4-8) \times 10^{-9}$ M). A high-affinity binding site (K_d of $\approx 7 \times 10^{-11}$ M) was not found on all cells to the same extent. The binding to the high-affinity site correlates well with data obtained for heregulin binding to breast carcinoma cells ($\sim 10^{-10}$ M) (16). The strongest indication of high-affinity binding was found for BT20-HER2 (Figure 5A,B). Similar binding data with a less pronounced high-affinity component were obtained for MCF-7 and BT474. MDA-MB231-HER2 cells exhibited very few high-affinity sites (Figure 5A,C), as would be expected on the basis of a relatively low density of HER4 and HER3 receptors (Table

1). Therefore, the near absence of high-affinity sites correlates with a lack of sensitivity on the part of MDA-MB231-HER2 cells, but the relative sensitivity of the responsive cell lines does not correlate directly with toxin binding. This would indicate that the presence of high-affinity binding sites is necessary, but not sufficient, to give maximum sensitivity toward the toxin.

To characterize further the nature of the high-affinity interaction of DT(389)hrg with the target cell, we carried out a competition experiment with free hrg (Figure 5D). In this analysis, DT(389)hrg is as potent as free hrg in displacing ¹²⁵I-DT(389)hrg from the high-affinity binding site. Taken together, these findings indicate that the hrg domain binds to the same target as the free hrg domain with comparable affinity. Any differences in toxin activity relative to other reported hrg toxin constructs are therefore not due to a reduced binding affinity of the hrg domain in the context of the chimeric toxin.

For a DT chimera to kill a target cell, the toxin must be endocytosed, since the acidic environment of the endosome is required to trigger the translocation of the catalytic domain of DT (31). To investigate whether the differences in cytotoxicity between cell lines with similar DT(389)hrg binding properties are due to differences in the rate of internalization, we measured the rate of ¹²⁵I-DT(389)hrg uptake (Figure 6). For this analysis, internalized counts per minute (cpm) have been normalized for cpm bound at the beginning of the experiment and do not reflect differences in the number of available receptors. A plot of internalized cpm without normalization (data not shown) shows that the four cell lines maintain the same order of internalization rates, but BT20-HER2 internalization rates are increased, which is consistent with the larger number of high-affinity binding sites found in our direct-binding studies. The four cell lines tested show marked differences in their rate of internalization. The time required for a 100% turnover ranges from 28 min for BT474 to 43–48 min for BT20-HER2 and MCF-7, respectively. The turnover observed for MCF-7 cells is also on the same time scale as the decrease in phosphorylated receptor in Figure 3a, following stimulation with DT(389)-hrg. In contrast, MDA-MB231 requires 2 h for a complete turnover. A down regulation to 74% (BT474) or 40–47% (BT20-HER2, MCF-7) of the initial internalization rate occurs within 4 h. Previous studies, using chimeras of the extracellular domain of the EGF receptor and the cytoplasmic domain of HER2, HER3, and HER4, have shown that the HER receptors are endocytosis-deficient relative to the EGF

receptor, which is rapidly internalized upon activation (32). The internalization and down regulation rates observed in our analysis are similar to those reported by Baulida et al. (32). MDA-MB231-HER2, which presents few high-affinity receptors according to our binding study, also exhibits a slow receptor internalization. Both combined features result in the lack of response to the chimeric toxin. Table 1 compares the different cell lines and summarizes the toxicity and internalization results.

DISCUSSION

We have analyzed two designs of chimeric toxins, consisting of the EGF-like domain of heregulin $\beta 1$ and a truncated form of diphtheria toxin, for their ability to act as directed toxins toward HER receptor overexpressing cell lines. These two designs differ in the placement of the hrg domain relative to the catalytic and translocation domains of DT (Figure 2), placing hrg either at the N terminus (hrg-DT(389)) or at the C terminus (DT(389)hrg) of DT(389).

Our data indicate that the placement of hrg at the C terminus of DT(389) does generate a functional, hrg-directed toxin. The DT(389)hrg construct is stable during purification, and access to the receptor-binding N terminus of hrg is not blocked by the fusion to the C terminus of DT(389). The ability of the hrg domain to bind its cognate receptor without interference is apparent from three different lines of evidence. The ability of DT(389)hrg to elicit ligand-dependent tyrosine phosphorylation of HER2 in less than 5 min of stimulation (Figure 3) demonstrates qualitatively that the hrg domain in DT(389)hrg can bind to its cognate receptor. Quantitatively, direct-binding studies indicate a high-affinity binding site with a K_d of approximately 7×10^{-11} M (Figure 5), a value comparable to that of free hrg (16). Furthermore, DT(389)hrg and hrg are equally potent in displacing labeled DT(389)hrg from this high-affinity site. The hrg-dependent cytotoxicity of DT(389)hrg was confirmed in two different assays on the basis of overall cytotoxicity (Figure 4) and the inhibition of protein synthesis (data not shown).

Placement of hrg at the N terminus of DT(389) does not result in a functional directed toxin. We observed growth stimulation in hrg-sensitive cell lines as well as cytotoxicity at the level of the DT(389) control (Figure 4). The experiments carried out on this construct are not sufficient to give an unambiguous explanation for the lack of directed cytotoxicity. One possible explanation could be that hrg-DT(389) is rapidly degraded in cell culture, resulting in the formation of free hrg and DT(389). During purification, this construct had a pronounced tendency for proteolysis (Figure 2B). Alternatively, the hrg domain could interfere with the translocation of the N-terminal fusion protein from the endosomal compartment to the cytosol. An example for such interference is provided by experiments in which dihydrofolate reductase (DHFR) was fused to the N terminus of DT. The fusion protein was translocated in the absence of methotrexate, but translocation was inhibited by the tight structure imposed on DHFR by methotrexate (33). The very compact nature of the hrg domain with its three internal disulfide bonds might pose a similar N-terminal block to successful translocation of the C domain to the cytosol.

Further analysis of the relative sensitivity of selected cell lines toward the functional directed toxin, DT(389)hrg, shows that the results obtained in this study are consistent with

previously published data on hrg-PE40 toxicity (18–20). On the basis of these studies, the expression of HER4, and to a lesser extent HER3, is required to achieve sensitivity to hrg-directed *pseudomonas* exotoxin A. The same dependency on HER4 or HER3 was found by Kihara et al. when a NIH/3T3 cell line transfected with EGFR, HER2, HER3, or HER4 was used as a constant cell background (20). HER2 overexpression alone is not sufficient to render cells sensitive. A comparison of the cytotoxicity assays (Figure 4) and direct-binding studies with DT(389)hrg (Figure 5) also indicates that the presence of a high-affinity binding site ($K_d \approx 7 \times 10^{-11}$ M) is required for sensitivity. Such a high affinity binding site would be provided by heterodimers of HER3 or HER4 with HER2. The direct-binding data, the expression levels of the different HER receptors (Table 1), and the sensitivity toward DT(389)hrg are therefore consistent with a requirement for HER4 or HER3 expression for hrg-directed cytotoxicity.

We attempted to correlate the presence of high-affinity sites with the observed differences in sensitivity between responsive cell lines. However, for those cell lines possessing high-affinity sites, the relative sensitivity toward DT(389)hrg does not correlate directly with the number of binding sites. A better correlation exists with the rate of internalization (Figure 6), indicating that high-affinity binding sites are required, but not sufficient, to achieve sensitivity to the toxin. This correlation with internalization rates could explain published results for some cell lines, which bind directed toxins such as DT(389)FGF or hrg-PE40 and exhibit receptor activation but fail to show cytotoxic effects (9, 30). However, it has to be noted, that for toxin sensitive cell lines, a 22-fold difference in toxicity is only matched by a less than 2-fold difference in the rate of normalized internalization. This would indicate that other unidentified factors further modulate the susceptibility to DT(389)hrg. Such factors could be unrelated to DT(389)hrg uptake and availability or could be linked to downstream events following internalization such as intracellular vesicle trafficking or protein degradation.

In addition to a comparison in the relative toxin sensitivity of different cell lines, an attempt can be made to compare the potency of DT(389)hrg with hrg-PE40 constructs. A direct comparison of IC(50) values for DT(389)hrg and hrg-PE40 has to be approached with caution, as the cells used for the analysis are not directly comparable and/or are derived from a different stock. Specifically, the hrg-PE40 data listed for comparison were derived from the parental and not from HER2 overexpressing cell lines. Keeping this in mind, the potency of the DT(389)hrg constructs seems to be slightly reduced compared to published values for hrg-PE40 (Table 1). The difference ranges from a 5-fold (BT20-HER2) to a 50-fold lower activity (BT474) of DT(389)hrg. There are several possible explanations for this difference in activity.

As previously mentioned, chimeric toxins based on PE40 place hrg at the N terminus and increase the accessibility of the ligand for receptor binding. The difference in potency could reflect a difference in receptor binding. However, the binding data for DT(389)hrg (Figure 5A–C) and the results of the competition experiment with free hrg (Figure 5D) rule out the explanation that reduced receptor-binding might be the cause for this reduced activity.

Translocation from the endosome to the cytosol does present another limiting step once endocytosis has occurred.

The mode of translocation of DT is still an area of intense investigation, but DT is thought to translocate from an early acidified endosome while *Pseudomonas* exotoxin A translocation probably involves early compartments of the secretory pathway (34). Furthermore, DT translocation can be inhibited by disulfide bonds inside the catalytic domain, while the exposed disulfide bond between the C and T domains is reduced under the acidic conditions of the endosome (35). This environment-dependent cleavage of disulfide bonds in the acidic endosome could negatively impact the translocation of DT(389)hrg. Additional factors that influence the effectiveness of DT fusions are the rate of subunit dissociation and channeling to the lysosomal compartment (36). These factors will likely differ from construct to construct.

In summary, we have analyzed two different designs for directed toxins based on truncated diphtheria toxin and the hrg domain. The replacement of the receptor-binding domain with hrg did yield a functional toxin which shows cell line specific cytotoxicity that is consistent with heregulin specificity. Cytotoxicity is not mediated by HER2 overexpression alone and appears to be dependent on high-affinity binding through HER3 and HER4 receptors. The level of cytotoxicity correlates best with the rate of internalization for cell lines exhibiting high-affinity binding sites. Since overexpression of HER2 is associated with a poor prognosis in more than 30% of human breast carcinoma and a number of other solid tumor malignancies, the development of potent directed toxins, aimed more specifically at HER2, is an important goal. The small and compact nature of the hrg domain makes it an ideal starting point for the development of small, HER2-specific ligands. The current toxin, DT(389)hrg, presents a functional and well-characterized system for analyzing and exploiting such changes in hrg specificity.

ACKNOWLEDGMENT

We thank Malgorzata Beryt (UCLA) for her help in all cell culture related experiments and Dr. David Reese (UCLA) for helpful advice and the sharing of information about the different cell lines used in our experiments. Special thanks to Dr. John R. Murphy (Boston University) for providing the C7hm723(β -tox) M8 strain of crm45-producing *C. diphtheriae* and Dr. John Collier (Harvard University) for his helpful advice in the design of experiments.

REFERENCES

- Gottstein, C., Winkler, U., Bohlen, H., Diehl, V., and Engert, A. (1994) *Ann Oncol.* 5 (Suppl. 1), 97–103.
- Kreitman, R. J., and Pastan, I. (1994) *Adv. Pharmacol.* 28, 193–219.
- Murphy, J. R., and vanderSpek, J. C. (1995) *Semin. Cancer Biol.* 6, 259–67.
- Choe, S., Bennett, M. J., Fujii, G., Curmi, P. M., Kantardjieff, K. A., Collier, R. J., and Eisenberg, D. (1992) *Nature* 357, 216–22.
- Naglich, J. G., Metherall, J. E., Russell, D. W., and Eidels, L. (1992) *Cell* 69, 1051–61.
- Myers, D. A., and Villemez, C. L. (1989) *Biochem. Biophys. Res. Commun.* 163, 161–4.
- Lakkis, F., Steele, A., Pacheco, S. A., Rubin, K. V., Strom, T. B., and Murphy, J. R. (1991) *Eur. J. Immunol.* 21, 2253–8.
- Murphy, J. R., Williams, D. P., Bacha, P., Bishai, W., Waters, C., and Strom, T. B. (1988) *J. Recept. Res.* 8, 467–80.
- Batoz, M., Fresno, P. M. C., Pizette, S., Raffioni, S., Birnbaum, D., and Coulier, F. (1995) *Cell Growth Differ.* 6, 1143–9.
- Tzahar, E., Levkowitz, G., Karunagaran, D., Yi, L., Peles, E., Lavi, S., Chang, D., Liu, N., Yayon, A., Wen, D. Z., and Yarden, Y. (1994) *J. Biol. Chem.* 269, 25226–33.
- Slamon, D. J., Godolphin, W., Jones, L. A., Holt, J. A., Wong, S. G., Keith, D. E., Levin, W. J., Stuart, S. G., Udove, J., Ullrich, A., and Press, M. (1989) *Science* 244, 707–12.
- Earp, H. S., Dawson, T. L., Li, X., and Yu, H. (1995) *Breast Cancer Res. Treat.* 35, 115–32.
- Marchionni, M. A., Goodearl, A. D., Chen, M. S., Bermingham-McDonogh, O., Kirk, C., Hendricks, M., Danehy, F., Misumi, D., Sudhalter, J., Kobayashi, K., Wroblewski, D., Lynch, C., Baldassare, M., Hiles, I., Davis, J. B., Hsuan, J. J., Totty, N. F., Otsu, M., McBurney, R. N., Waterfield, M. D., Stroobant, P., and Gwynne, D. (1993) *Nature* 362, 312–8.
- Carraway, K. L. r., Weber, J. L., Unger, M. J., Ledesma, J., Yu, N., Gassmann, M., and Lai, C. (1997) *Nature* 387, 512–6.
- Chang, H., Riese, D. J. n., Gilbert, W., Stern, D. F., and McMahon, U. J. (1997) *Nature* 387, 509–12.
- Holmes, W. E., Sliwkowski, M. X., Akita, R. W., Henzel, W. J., Lee, J., Park, J. W., Yansura, D., Abadi, N., Raab, H., Lewis, G. D., Shepard, H. M., Kuang, W. J., Wood, W. I., Goeddel, D. V., and Vandlen, R. L. (1992) *Science* 256, 1205–10.
- Barbacci, E. G., Guarino, B. C., Stroh, J. G., Singleton, D. H., Rosnack, K. J., Moyer, J. D., and Andrews, G. C. (1995) *J. Biol. Chem.* 270, 9585–9.
- Fiddes, R. J., Janes, P. W., Sanderson, G. M., Sivertsen, S. P., Sutherland, R. L., and Daly, R. J. (1995) *Cell Growth Differ.* 6, 1567–77.
- Jeschke, M., Wels, W., Dengler, W., Imber, R., Stücklin, E., and Groner, B. (1995) *Int. J. Cancer* 60, 730–9.
- Kihara, A., and Pastan, I. (1995) *Cancer Res.* 55, 71–7.
- Bennett, M. J., Choe, S., and Eisenberg, D. (1994) *Protein Sci.* 3, 1444–63.
- Louie, L. V., Yang, W., Bowman, M. E., and Choe, S. (1997) *Mol. Cell* 1, 67–78.
- Nagata, K., Kohda, D., Hatanaka, H., Ichikawa, S., Matsuda, S., Yamamoto, T., Suzuki, A., and Inagaki, F. (1994) *EMBO J.* 13, 3517–23.
- Stenmark, H., Moskaug, J. O., Madhus, I. H., Sandvig, K., and Olsnes, S. (1991) *J. Cell. Biol.* 113, 1025–32.
- Pegram, M. D., Finn, R. S., Arzoo, K., Beryt, M., Pietras, R. J., and Slamon, D. J. (1997) *Oncogene* 15, 537–47.
- Flick, D. A., and Gifford, G. E. (1984) *J. Immunol. Methods* 68, 167–75.
- Carroll, S. F., and Collier, R. J. (1988) *Methods Enzymol.* 165, 218–25.
- Gordon, V. M., Klimpel, K. R., Arora, N., Henderson, M. A., and Leppla, S. H. (1995) *Infect. Immun.* 63, 82–7.
- Graus-Porta, D., Beerli, R. R., and Hynes, N. E. (1995) *Mol. Cell Biol.* 15, 1182–91.
- Siegall, C. B., Bacus, S. S., Cohen, B. D., Plowman, G. D., Mixan, B., Chace, D., Chin, D. M., Goetze, A., Green, J. M., Hellstrom, I., Hellstrom, K. E., and Fell, H. P. (1995) *J. Biol. Chem.* 270, 7625–30.
- Draper, R. K., and Simon, M. I. (1980) *J. Cell. Biol.* 87, 849–54.
- Baulida, J., Kraus, M. H., Alimandi, M., Di Fiore, P. P., and Carpenter, G. (1996) *J. Biol. Chem.* 271, 5251–7.
- Klingenberg, O., and Olsnes, S. (1996) *Biochem. J.* 313, 647–53.
- Simpson, J. C., Dascher, C., Roberts, L. M., Lord, J. M., and Balch, W. E. (1995) *J. Biol. Chem.* 270, 20078–83.
- Falnes, P. O., and Olsnes, S. (1995) *J. Biol. Chem.* 270, 20787–93.
- Chang, T. M., Hossain, A., and Chang, C. H. (1994) *Biochim. Biophys. Acta* 1224, 77–88.
- Rees, D., Arboleda, J., Twaddell, J., Akita, R., Sliwkowski, M., and Slamon, D. (1996) *Proc. Am. Assoc. Cancer Res.* 37, 51.
- Kraulis, P. J. (1991) *J. Appl. Crystallogr.* 24, 946–50.